This article has been accepted for publication in IEEE Transactions on Multimedia. This is the author's version which has not been fully edited and content may change prior to final publication. Citation information: DOI 10.1109/TMM.2022.3187607

A Machine Learning Solution for Video Delivery to Mitigate Co-Tier Interference in 5G HetNets

Devanshu Anand, Mohammed Amine Togou, and Gabriel-Miro Muntean

School of Electronic Engineering, Dublin City University, Ireland

***Abstract*—The exponential demand for multimedia services is one reason behind the substantial growth of mobile data traffic. Video traffic patterns have significantly changed in the past two years due to the coronavirus disease (COVID-19). The worldwide pandemic has caused many individuals to work from home and use various online video platforms (*e.g.,* Zoom, Google Meet, and Microsoft Teams). As a result, overloaded macrocells are unable to ensure high Quality of Experience (QoE) to all users. Heterogeneous Networks (HetNets) consisting of small cells (femtocells) and macrocells are a promising solution to mitigate this problem. A critical challenge with the deployment of femtocells in HetNets is the interference management between Macro Base Stations (MBSs), Femto Base Stations (FBSs), and between FBS and FBS. Indeed, the dynamic deployment of femtocells can lead to co-tier interference. With the rolling out of the 5G mobile network, it becomes imperative for mobile operators to maintain network capacity and manage different types of interference. Machine Learning (ML) is considered a promising solution to many challenges in 5G HetNets. In this paper, we propose a Machine Learning Interference Classification and Offloading Scheme (MLICOS) to address the problem of co-tier interference between femtocells for video delivery. Two versions of MLICOS, namely, MLICOS1 and MLICOS2, are proposed. The former uses conventional ML classifiers while the latter employs advanced ML algorithms. Both versions of MLICOS are compared with the classic Proportional Fair (PF) scheduling algorithm, Variable Radius and Proportional Fair scheduling (VR+PF) algorithm, and a Cognitive Approach (CA). The ML models are assessed based on the prediction accuracy, precision, recall and F-measure. Simulation results show that MLICOS outperforms the other schemes by providing the highest throughput and the lowest delay and packet loss ratio. A statistical analysis was also carried out to depict the degree of interference faced by users when different schemes are employed.**

***Index Terms*- HetNets, COVID-19, Interference, Machine Learning, QoS, Statistical Visualization**

I. Introduction

Recently, user demand for cellular data has surged due to the rapid increase in the number of both smart devices and mobile applications. Video streaming applications, including video on demand and live streaming, account for the majority of mobile data traffic. According to Cisco [1], video traffic has increased at a compound rate of 26% from 2016 to 2020, and will account for 82% of all Internet traffic by the end of 2022. As video traffic and applications are increasing exponentially, the need for good resource management is of paramount importance, especially in indoor spaces. Radio signals in indoor environments are relatively weak due to aspects such as path loss and fast fading. This indicates that sometimes the bandwidth shared by users from Macro Base Stations (MBS) is insufficient to support the delivery of high quality multimedia content [2]. At other times, reliable and fast delivery of multimedia content is of great significance for the service provided [3]. In general, video streaming services have high bandwidth and tight timing requirements, sometimes exceeding the network support. This calls for an efficient way to deliver videos, specific to ultradense HetNets [4].

One promising solution to improve the overall network capacity is to provide 5G support as part of HetNets. HetNets consist of small cells that are deployed within the macro cell coverage area. Among the small cell solutions (*i.e.,* femtocells, microcells, and picocells), femtocells have recently received considerable attention in the new 5G service-based architecture. Femtocells do not face any challenges related to site availability, as users install FBS themselves and use existing user broadband connections. They also introduce very little overhead on mobile operators [5]. A femtocell provides three types of access modes to its users. Open access allows access to all User Equipment (UE) with no restriction, while the closed access mode enables access only to authorized users. The hybrid access enables access to authorized UEs along with a limited number of predefined UEs in a prioritized manner. A femtocell helps improve the indoor radio signal quality, operates on a licenced spectrum, and provides good wireless access service.

Due to limited radio resources, a femtocell shares the same licenced range with a macrocell in the traditional cellular network, leading to signal interference. The interference between the macrocell and femtocell is called cross-tier interference. The dynamic deployment of multiple femtocells also determines a intercell interference known as co-tier interference, which is one of the primary concerns with femtocell deployment in HetNets. In an ideal HetNet, co-tier interference can be minimized if femtocells are deployed with appropriate planning. However, due to the plug and play feature of femtocells, co-tier interference occurs even after appropriate planning. In HetNets, there will always be more femtocells than macrocells and a high number of femtocells helps reduce the load of the macrocells. However, such a setup introduces interference, in particular co-tier interference and it is important to address it to ensure good QoS levels and high user QoE.

All major video content providers (*e.g.,* YouTube, Youku, Netflix) have made great efforts to deliver the most exciting content to users [6]. They require an increased amount of bandwidth, which calls for the use of femtocells in a HetNet environment. Femtocell employment results in interference,

This article has been accepted for publication in IEEE Transactions on Multimedia. This is the author's version which has not been fully edited and content may change prior to final publication. Citation information: DOI 10.1109/TMM.2022.3187607

which ultimately affects the quality of service (QoS) of the delivered content. Therefore, there is an important need to mitigate the co-tier interference and ensure good quality of the delivered multimedia content in HetNets.

Following considerable research efforts, many schemes have been proposed to minimize the effect of co-tier interference in HetNets, including clustering techniques, cognitive approaches, resource allocation solutions and power control techniques [7][8][9][10]. Among them, Sultan et al. [11] discussed power and radio resource management techniques to mitigate the co-tier interference in femtocells. However, their proposed scheme measured the level of interference for each femtocell only. Tian et al. [12] introduced a cognitive interference management technique for the Internet of Things (IoT) in a two-tier network. Pyun et al. [13] proposed a heuristic optimization resource allocation scheme to mitigate co-tier interference during uplink transmissions in femtocell networks. Dai et al. [14] introduced an interference management technique based on resource allocation and a common clustering method in order to mitigate co-tier interference in an Orthogonal Frequency Division Multiplexing (OFDM)-based femtocell network. All different schemes from the literature have proposed good unique solutions to mitigate co-tier interference. However, as these methods cannot be used in an online mode, novel techniques are sought, including using ML [15].

This paper proposes the **Machine-Learning Interference Classification and Offloading Scheme, MLICOS**, a ML-based solution for the co-tier interference problem during video delivery in HetNets. The proposed solution involves a novel machine learning-based interference classification algorithm and an offloading scheme applied on the most affected traffic to mitigate the co-tier interference between the femtocells and improve QoS levels.

Fig. 1 illustrates the two-tier HetNet environment deployment for video delivery considered in this work. It involves multiple femtocells and one macrocell. We assume femtocells employ the closed access mode. The proposed MLICOS scheme gives femtocells a cognitive sense that helps classify users based on the interference level they experience. MLICOS selects the most affected users and offloads their traffic to nearby FBS, reducing the co-tier interference and improving the overall QoS. The ML algorithms used by MLICOS are assessed in terms of prediction accuracy, precision, recall and F-measure. Two versions of MLICOS are proposed, namely, MLICOS1 and MLICOS2. MLICOS1 uses the conventional ML algorithms and MLICOS2 uses the neural network algorithms. Both versions are tested in the simulated HetNet and their performance is compared with that of other state-of-the-art solutions based on QoS metrics such as throughput, delay and Packet Loss Ratio (PLR).

The main contributions of this paper are as follows:

1) We propose a ML solution to address the problem of co-tier interference. The proposed solution has two stages. The first classifies the users based on the interference level, while the second offloads users from the high interference class to nearby FBS.

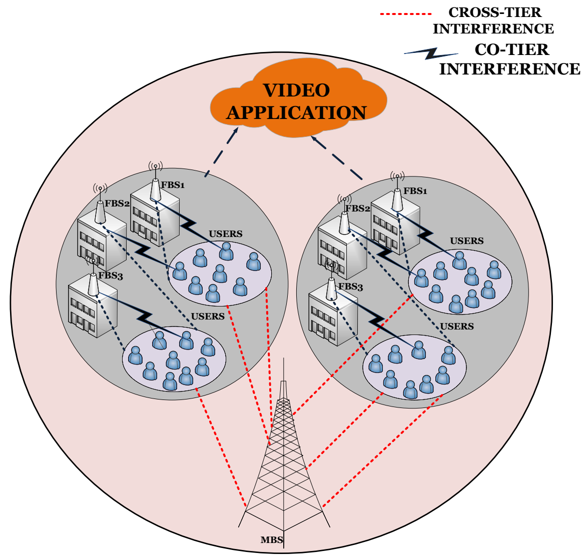

Fig. 1: An example of a two-tier HetNet, including one MBS and several FBS, located in residential buildings that constitute hotspots for wireless traffic. In this scenario, most UE is streaming videos, while the rest is generating regular web traffic. UE in a given region is either served by MBS or FBS, which can lead to co-tier and cross-tier interference, affecting QoS and user QoE.

2) We perform an in-depth performance analysis of the proposed versions of MLICOS against three other schemes, demonstrating the proposed solution's superiority.

The rest of the paper is organized as follows. Section II surveys some related works. Section III formulates the problem. The system model and proposed MLICOS algorithm are presented in Section IV. Performance evaluation, including ML analysis, QoS assessment and result visualization and analysis, is discussed in Section V. Finally, Section VI concludes the paper and indicates some future research directions.

II. Related Works

A HetNet may involve a large number of UEs and access points, making it challenging to meet the delay-sensitive QoS demands for video applications and services. In addition, the dynamic deployment of femtocells in HetNets may lead to co-tier interference, which can reduce overall network capacity. There are an abundant number of interference management schemes and techniques that have been proposed in the literature. In this section, we briefly review some of the existing co-tier interference management techniques. They are organized into four different categories: clustering techniques, cognitive approaches, resource allocation schemes, and power control techniques.

A. Clustering Techniques

Clustering techniques identify similarities between users based on vicinity, power, and cell-clustering policy, and group them according to those characteristics that are common. These groups are known as ”clusters”. In [16], the authors

This article has been accepted for publication in IEEE Transactions on Multimedia. This is the author's version which has not been fully edited and content may change prior to final publication. Citation information: DOI 10.1109/TMM.2022.3187607

proposed a semi clustering of a victim-cell (SCVC) approach, which clusters users based on UEs status (*i.e.,* critical and non critical), and accordingly, assigns resource blocks among the various clusters. This helps to manage the co-tier interference. In [17], the authors divided the problem into two subproblems. First, a femtocell clustering scheme based on LINGO for mathematical modelling was used. Second, a novel algorithm was proposed to allocate subchannels to femtocell users. The proposed algorithm predicts the change tendency of the path loss values of UEs. A clustering approach that groups users and femtocells based on line of sight connectivity was introduced in [18], while Wang *et al.* [19] proposed a Data-Driven Power Control (DDPC) technique based on an Affinity Propagation (AP) clustering algorithm. It clusters the various femtocells based on the reference signal received power (RSRP). In [20], the authors proposed a dynamic cell clustering-based resource algorithm to mitigate co-tier interference in femtocells. The proposed algorithm includes two steps, one for assigning subchannels for users and the second helps mitigate the interference by controlling the power. In [21], the authors proposed a small cell power control algorithm (SPC) and interference-managed hybrid clustering (IMHC) scheme, to resolve the issue of co-tier and cross-tier interference in the small cell base station cluster tiers. The proposed scheme improved the system throughput with reduced interference but did not considered other QoS metrics, such as jitter, PLR and delay. In [22], the authors proposed an interference management technique to mitigate the problem of co-tier interference in ultra dense small cell networks. It deploys a clustering-based interference management scheme in which the subchannel resources are allocated in the process of cluster generation. While clustering techniques find common characteristics and group users into different clusters, classification algorithms use predefined classes to which users are assigned.

B. Cognitive Approaches

Cognitive approaches have been proposed for a long time in the literature to mitigate co-tier interference. Tian *et al.* [12] proposed a cognitive technique for a network of femtocells serving multiple IoT devices. The authors described two cognitive Interference Alignment (IA) schemes. The first offers a nulling-based IA scheme that aligns the co-tier interference into the orthogonal subspace at each IoT receiver. The second presents a partial cognitive IA scheme that further enhances the network performance with low signal to noise ratio v alues. Zhang *et al.* [23] proposed a cognitive approach to mitigate co-tier interference in femtocells. In the proposed scheme, a FBS allocates component carriers to its UE for transmission. The UE uses RSRP values to perform path loss measurements from its FBS and neighbouring FBS. If the RSRP value is low on one of the component carriers, the FBS selects that component carrier as the primary to help reducing the co-tier interference. Similarly, a Cognitive Radio Femtocell Base Station (CFBS) was proposed in [24]. The CFBS constructs a radio environment map (REM) by sensing the radio environment. The REM is used to assign resources to authorized users and therefore helps mitigate interference. A dynamic algorithm based on a distance-based approach was proposed in [25]. It minimizes the interference in a Device-to-Device (D2D) enabled cellular network and guarantees QoS for both cellular and D2D communication links. Finally, Wang *et al.* [26] used a cognitive relay to increase the capacity of femtocell users and avoid co-tier interference among femtocells.

C. Resource Allocation

Resource allocation techniques basically help allocate resources in an efficient manner in HetNets, along with reducing the co-tier interference. In [27], the authors proposed a statistical resource allocation scheme that helps mitigate the cross-tier, co-tier and cross-link interference in ultra-dense heterogeneous networks. They considered Time Division Duplex (TDD) mode for uplink and downlink transmission, which can lead to cross-slot interference. This can be avoided by using the Frequency Division Duplex (FDD) mode. In [28], the authors proposed a Variable Radius algorithm for the enhanced distribution of resources and interference management in a LTE femtocell network. The scenario considered the femtocell's open access mode, where all users are authorized to connect to the femtocell network. In [29], the authors described a bat algorithm based on the nearest-integer discretization method to minimize the interference in a closed access femtocell network. In [30], the authors analyzed the issue of resource allocation in 5G networks by classifying the various proposed resource allocation schemes and assessing their ability to enhance service quality. In [31], the authors considered the hybrid access mode in a FBS deployment scenario and proposed a resource allocation technique based on a cuckoo search algorithm, RACSA, for cross-tier interference mitigation in Orthogonal Frequency Division Multiple Access-based Long Term Evolution (OFDMA-LTE) system.

D. Power Control Techniques

Chen *et al.* [32] proposed a threshold-based handover algorithm to mitigate co channel interference in a two-tier femtocell network. The proposed scheme considers a Signal to Interference and Noise Ratio (SINR) value as the threshold to manage the transmission power of the FBS. Unfortunately, only the uplink co channel interference was considered. In [33], the authors proposed two power control methods to reduce the interference effect in a two-tier network using SINR. Both methods were able to mitigate well the impact of interference by controlling the transmission power. An Active Power Control (APC) technique was proposed in [34], which helps to reduce the intercell interference and reduces wastage of unnecessary power consumption in a green femtocell network. In [35], the authors proposed a soft frequency reuse (SFR) scheme to minimize the interference and increase the network throughput. The proposed scheme solves the interference problem of densely deployed SCs by dividing the cell region into centre and edge zones. The proposed scheme is based on n on/off switches, which tackles the elevated power consumption problem and enhances the power efficiency of 5G networks. In [36], Stackelberg game theory was used to formulate a power control scheme that mitigates interference in a shared spectrum two-tier network. The proposed scheme was compared with the baseline scheme, where a two-way pricing mechanism was integrated into the Stackelberg game to reduce the co-tier interference among femtocells.

The schemes mentioned from the research literature help mitigate co-tier interference among femtocells. To the best of our knowledge, no ML-based solution has been proposed to assess the level of interference faced by users when delivering multimedia content and address the co-tier interference problem in a 5G HetNets. This paper proposes a scheme that considers video content to be delivered among femtocell users and mitigates co-tier interference, which impacts video delivery content by making efficient use of resources while maintaining high QoS values in 5G HetNets.

III. Problem Formulation

We consider a heterogeneous network environment consisting of a set of MBSs M = $\{M_1, M_2, M_3, ..., M_m, ..., M_{N_m}\}$ and a set of FBSs F = $\{F_1, F_2, F_3, ..., F_f, ..., F_{N_f}\}$, within the coverage area of the MBSs. A simplified version of the network scenario with a single MBS is illustrated in Fig. 1. We assume that users are randomly allocated to the nearest FBS. Let U denote a set of UEs that is randomly and uniformly distributed: U = $\{u_1, u_2, u_3 ....u_i, ..., u_{N_u}\}$.

The communication quality in the context of existing interference between user u_i and F_f, in the coverage area of M_m, is measured by $\alpha_{i,f}$, computed as follows:

$$\alpha_{i,f} = \frac{P_i^f G_i^f}{{N_o}^2 + \sum_{u_j \epsilon U} {P_j}^m {G_j}^m + \sum_{u_j \epsilon U} {P_j}^f {G_j}^f} \quad (1)$$

where P_i^f and P_j^m denote the transmission power of UEs relative to F_f and M_m, respectively. ${G_i}^f$ denotes the gain of the channel between u_i and the allocated F_f while ${G_j}^m$ designates the gain of the channel between u_j and the allocated M_m. N_o is the channel's average white noise power. Similarly, the communication quality in the presence of interference between user u_i and M_m is expressed as follows:

$$\alpha_{i,m} = \frac{P_i^m G_i^m}{{N_o}^2 + \sum_{u_j \epsilon U} {P_j}^m {G_j}^m + \sum_{u_j \epsilon U} {P_j}^f {G_j}^f} \quad (2)$$

The maximum achievable throughput by the network can be expressed by Shannon's Law and is given by:

$$Thr = \sum_{u_i \epsilon U} (B_i^f \log_2(1 + \alpha_{i,f}) + B_i^m \log_2(1 + \alpha_{i,m})) \quad (3)$$

where Thr is the sum of throughput in the network, and B_i^f and B_i^m are the bandwidths available for user u_i when associated with FBS F_f and MBS M_m, respectively.

The total round trip delay experienced by a packet exchanged between user u_i and FBS F_f can be expressed as follows:

$$D_{i,f} = D_{i,f}^t + D_{i,f}^{pr} + D_{i,f}^p + D_{i,f}^q \quad (4)$$

where, $D_{i,f}^t$ is the transmission delay, defined as the time it takes to transmit packets; $D_{i,f}^{pr}$ is the radio propagation delay, described as the time packets take to reach the receiver; $D_{i,f}^p$ is the signal processing delay, indicating the time to decode the packet at the receiver; and while $D_{i,f}^q$ is the queuing delay, specifying the packet waiting time in the buffer. If we assume that the radio propagation delay and signal processing delay are very small [37] and are negligible, the total round trip packet delay can be expressed as:

$$D_{i,f} = D_{i,f}^t + D_{i,f}^q \quad (5)$$

Similarly, the round trip delay experienced by a packet exchanged between u_i and MBS M_m can be computed as:

$$D_{i,m} = D_{i,m}^t + D_{i,m}^q \quad (6)$$

Thus, the mean delay values for user u_i are:

$$\bar{D}_{i,f} = \sum D_{i,f}/N_{i,f} \quad (7)$$

$$\bar{D}_{i,m} = \sum D_{i,m}/N_{i,m} \quad (8)$$

where $N_{i,f}$ and $N_{i,m}$ are the numbers of delay samples.

Assuming that loss is a random process that follows a Bernoulli distribution [38], [39], [40], the Packet Loss Rate (PLR) between FBS F_f and u_i is expressed as:

$$\sigma_{i,f} = \sqrt{X_{i,f} * Y_{i,f}/N_{i,f}} \quad (9)$$

where $X_{i,f}$ is the probability of dropping a packet, $Y_{i,f}$ is the probability of receiving a packet (can also be expressed as (1-$X_{i,f}$)) and $N_{i,f}$ is the total number of samples. Likewise, PLR between MBS M_m and u_i is expressed as:

$$\sigma_{i,m} = \sqrt{X_{i,m} * Y_{i,m}/N_{i,m}} \quad (10)$$

The problem described in this work has three goals: $G_1, G_2 and G_3$, expressed in terms of the following equations:

1) Maximize the network throughput, calculated according to Eq. (3):
$$G_1 = max(Thr) \quad (11)$$
2) Minimize the average packet delay across all users (calculated according to Eqs. (7) and (8):
$$G_2 = min\left(\left[\sum_{u_i \epsilon U} \bar{D}_{i,f} + \sum_{u_i \epsilon U} \bar{D}_{i,m}\right]/N_u\right) \quad (12)$$
3) Minimize the average PLR across all users (calculated according to Eqs. (9) and (10):
$$G_3 = min\left(\left[\sum_{u_i \epsilon U} \sigma_{i,f} + \sum_{u_i \epsilon U} \sigma_{i,m}\right]/N_u\right) \quad (13)$$

These goals are achieved by reducing the co-tier interference in the femtocell-enhanced network environment, thereby, improving the quality of the multimedia content delivery.

This article has been accepted for publication in IEEE Transactions on Multimedia. This is the author's version which has not been fully edited and content may change prior to final publication. Citation information: DOI 10.1109/TMM.2022.3187607

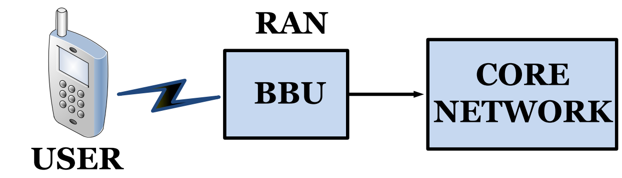

(a) Traditional Radio Access Network (RAN) Architecture

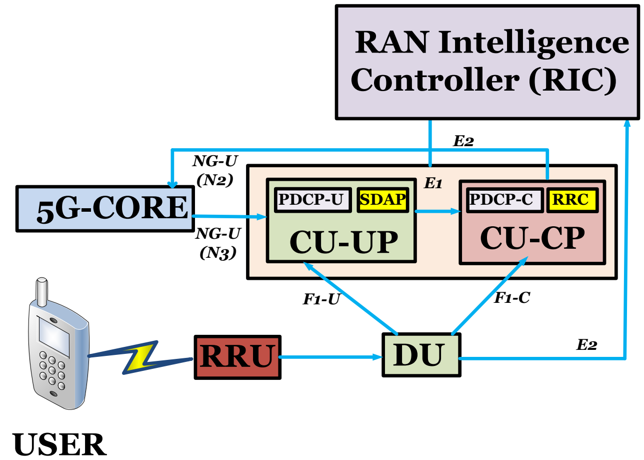

(b) O-RAN System Architecture

Fig. 2: RAN network supported in traditional 3G/4G and new 5G cellular networks

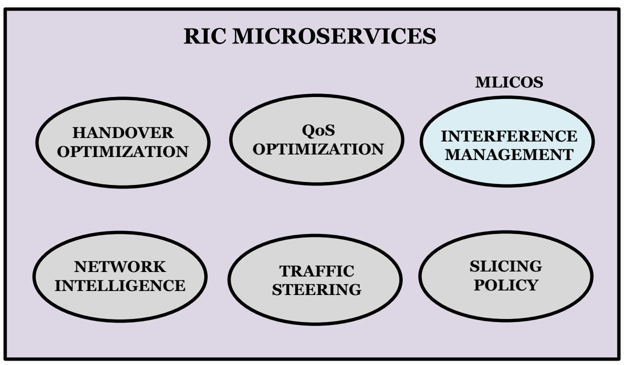

Fig. 3: MLICOS interference management service as part of the RIC microservices

IV. System Model

A. System Architecture

This paper considers an Open-Radio Access Network (O-RAN) architecture, supported in a 5G network environment [41]. Within the O-RAN architecture, the functions of the traditional RAN are split into multiple entities with open interfaces between them: Remote Radio Unit (RRU), Distributed Unit (DU) and Centralised Unit (CU). These entities can be developed by different vendors, allowing for flexibility.

Fig. 2a illustrates RAN components in a traditional network context. The traditional RAN is considered a black box in which the internal interfaces are closed and operated only by a single vendor. Fig. 2b shows the O-RAN-enhanced system architecture. According to the 3GPP standards, CU consists of a logical unit that integrates the Radio Resource Control (RRC), Service Data Adaptation Protocol (SDAP) and Packet Data Convergence Protocol (PDCP). These are a part of both the User Plane (UP) and Control Plane (CP). CP carries the signalling traffic and UP transports the user traffic. CU also controls the operations of one or multiple DUs, which are logical units that host Radio Link Control (RLC), Medium Access Control (MAC), and are partially controlled by the CU. RRU is integrated with the 5G MIMO antenna [42]. An essential part of this system architecture is the RAN Intelligence Controller (RIC) which contains various artificial intelligence (AI)/ML models that help improve network operations. AI/ML models situated in the RIC controller support many microservices, including handover optimization, QoS optimization, network slicing and interference management [43]. The proposed MLICOS is part of this intelligence (see Fig. 3).

As illustrated in Fig. 4, MLICOS includes an Interference Management Server (IMS) that acquires information on both co-tier and cross-tier interference in 5G HetNets. MLICOS focuses on co-tier interference and, as discussed, involves classification and traffic offloading. Classification identifies low co-tier interference users (C-1) and high co-tier interference users (C-2). MLICOS reduces the co-tier interference for C-2 users by offloading user traffic to the nearby FBS, depending upon the availability of resources at that particular FBS. The resource monitor keeps a track of resources at a particular FBS which helps in the offloading process. Traffic offloading is performed using a solution such as the one proposed in [44].

B. Machine Learning Interference Classification and Offloading Scheme (MLICOS)

The proposed approach is a ML solution that classifies users into two different classes based on the level of experienced co-tier interference within the FBS coverage area: low co-tier interference class (C-1) and high co-tier interference class (C-2). The MLICOS focuses on C-2 users and offloads their traffic to a nearby FBS to improve the QoS and QoE metrics for video streaming services.

The proposed algorithm has three phases, as shown in Algorithm 1: *Initialization*, *Classification*, and *Offloading*. In the *Initialization* phase and, U is the set of UEs, randomly and uniformly distributed. Let B_s be the set of all base stations as $B_s = \{B_1, B_2, \ldots, B_{N_m}, B_{N_{m+1}}, \ldots, B_t, \ldots, B_T\}$, where $T = N_m + N_f$. Let R^t be the available set of resource blocks at BS_t, defined as $R^t = \{r_1^t, r_2^t, ..., r_j^t, ..., r_{N_r^t}^t\}$, where N_r^t is the number of resource blocks at BS_t. We assume that the

This article has been accepted for publication in IEEE Transactions on Multimedia. This is the author's version which has not been fully edited and content may change prior to final publication. Citation information: DOI 10.1109/TMM.2022.3187607

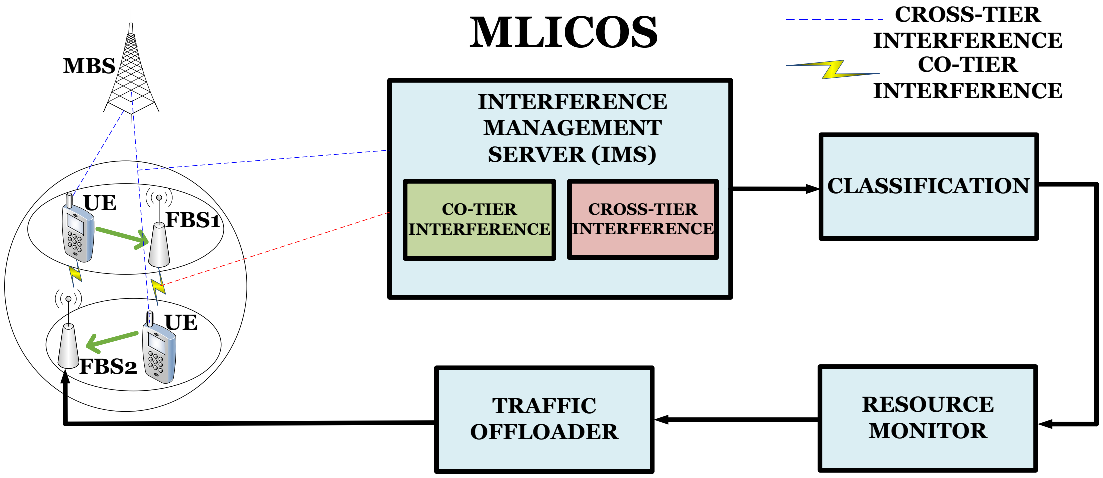

Fig. 4: MLICOS block architecture

Algorithm 1: MLICOS Algorithm

Goals: Increase Throughput (Thr), Decrease Delay (D_t) and PLR (σ)
Phase 1: **Initialization :**
1. N_u, $\forall u_i \in U$;
2. C1= {}, C2= {};
3. $B_s = \{B_1, \dots, B_t, \dots, B_T\}$;
4. Threshold α;
5. User Interference Matrix (UIM);
6. User Association Matrix (UAM);

Phase 2: Classification
foreach $u_i \in U$ **do**
  foreach $r_j^t \in N_r^t$ **do**
    if $UIM[i,j] < \alpha$ **then**
      $C_1 \leftarrow$C$_1 \cup \{u_i\}$
      user in the low co-tier interference class
    else if $UIM[i,j] \geq \alpha$ **then**
      $C_2 \leftarrow$C$_2 \cup \{u_i\}$
      user in the high co-tier interference class
    i++;
  end
end

Phase 3: Offloading
foreach $u_i \in C_2$ *AND* $B_t \in B_s$ **do**
  if $UAM[i,t] = 1$ **then**
    Compute S^i as in Eqs. (16);
    Determine s_g^i as in Eqs. (17);
    foreach $r_j^t \in N_r^t$ **do**
      Offload u_i to a new FBS B_g having the available resource blocks and which guarantees maximum throughput, lowest delay and PLR according to Eqs. (11), (12), and (13);
      Update UIM and UAM
    end
    ;
  i++;
end

resource blocks available at each BS $t \in B_s$ are the same. This assumption does not affect the generality of the solution. These resource blocks are further divided into subchannels and are assigned to the UEs associated with BS_t. In the *initialization* phase, two matrices are filled. They are defined as follows:

$$\mathbf{UIM} = \begin{bmatrix} UIM_{1,1} & \dots & UIM_{1,N_r^t} \\ UIM_{2,1} & \dots & UIM_{2,N_r^t} \\ \vdots & \ddots & \vdots \\ UIM_{N_u,1} & \dots & UIM_{N_u,N_r^t} \end{bmatrix} \tag{14}$$

The User Interference Matrix (UIM) is introduced in Eq. (14), where $UIM[i,j]$ indicates the effect of the interference experienced by u_i on resource block r_j^t. The interference effect is assessed using SINR values, which are calculated according to Eq. (1) with $UIM[i,j] = \alpha_{i,j}$.

$$\mathbf{UAM} = \begin{bmatrix} UAM_{1,1} & \dots & UAM_{1,B_T} \\ UAM_{2,1} & \dots & UAM_{2,B_T} \\ \vdots & \ddots & \vdots \\ UAM_{N_u,1} & \dots & UAM_{N_u,B_T} \end{bmatrix} \tag{15}$$

The User Association Matrix (UAM) is presented in Eq. (15), where $UAM[i,t]$ indicates the association of each u_i with one BS BS_t, which can be either the MBS or FBS. In this paper, we consider $UAM[i,t]$ as a binary variable. If u_i is not associated with BS_t, $UAM[i,t] = 0$; otherwise, $UAM[i,t] = 1$. Since this paper focuses on co-tier interference, we consider UEs that is associated with FBSs only ($t > N_m$). Both matrices are updated after each iteration. Note that we assume that only one user is associated with one resource block per time slot in each FBS. This assumption enables disregarding the interference between users within the same cell.

In the *classification* phase, we categorize users based on their experienced level of interference. In this paper, two levels are considered: *high (C-2)* and *low (C-1)*. We consider α as a threshold value for assessing of the interference between a user and a selected FBS. Using ML algorithms, users who experience interference above the threshold value α are assigned to C-2; the rest of the users are assigned to C-1. We tune the hyperparameters for the ML algorithms and then perform user classification. The novelty of the ML algorithms is shown in the second stage of Algorithm 1.

This article has been accepted for publication in IEEE Transactions on Multimedia. This is the author's version which has not been fully edited and content may change prior to final publication. Citation information: DOI 10.1109/TMM.2022.3187607

In the *offloading* phase, C-2 users are offloaded to a nearby FBS that has enough resource blocks to meet the user's requirements while also contributing to the achievement of goals G1, G2, and G3. To this end, we use the received signal strength to identify the most suitable FBS. We define the vector S^i as follows:

$$S^i = \{s_1^i, s_2^i, ..., s_f^i, ..., s_{N_f}^i\} \tag{16}$$

where s_f^i is the signal strength experienced by user u_i with respect to FBS F_f. We compute the signal strength for each C-2 user and offload the user's traffic to FBS g, which has the lowest signal strength and available resource blocks, as indicated in Eq. (17).

$$s_g^i = min\{s_f^i | \forall f, 1 \leq f \leq N_f\} \tag{17}$$

Note that by offloading users from macrocells to nearby femtocells, more resource blocks at the macrocell level are made available, which can be used to improve the QoS of users in C-1, and hence contribute to the realization of G1, G2, and G3. Additionally, note that offloading all C2 user traffic to new FBSs does not guarantee that there will be no interference; hence, the proposed scheme runs iteratively until all UIM values drop below α or in case no improvement has been achieved in the previous iterations.

C. Machine Learning-based Algorithm

We formulate the given challenge as a ML-based problem and use the binary classification method as a solution since it requires less training time and is usually faster to converge [45]. Fig. 5 illustrates the main components of the proposed solution. First, simulations are carried out using the Network Simulator NS-3. After each iteration, relevant data are saved in a Comma Separated Value (CSV) file and constitute our simulated dataset. The reason we opted for a simulated dataset is threefold: 1) we avoid any confidentiality and privacy liability that may arise from using a real-world dataset; 2) we know the environment used for generating the dataset. Therefore, we can easily make changes to simulation parameters along with hyperparameters of the ML models [46]; and 3) the generated dataset is specific to the scenario we are examining since it solely focuses on one type of traffic (*i.e.,* video traffic). The collected data contain values of the following parameters: SINR, RSRP, Reference Signal Received Quality (RSRQ) and cell ID. The CSV file is given as input in the Python environment for classification purposes. The first step is data preprocessing, which is required for replacing and eliminating nonnumeric or symbolic features from a dataset. Next, the feature selection stage helps eliminate noise in the data and focuses only on the relevant data in a dataset. For the ML models used by MLICOS, SINR is the target feature of interest. The dataset is split into 80% training data and 20% test data, which are used during training and testing of our proposed solution, respectively [47].

Two versions of MLICOS were designed: MLICOS1 and MLICOS2. MLICOS1 employs supervised ML techniques, mainly Support Vector Machine (SVM) and Random Forest (RF). While SVM is one of the best classifiers and is considered a benchmark in the field of statistical learning and ML [48], RF is an ensemble learning algorithm that can ensure high accuracy while handling multiple outliers in training and test datasets. MLICOS2 deploys two neural network approaches, Artificial Neural Network (ANN) and Convolutional Neural Network (CNN) [49]. The ANN and CNN used a three-layer neural network structure composed of input, hidden and output layers. We employed the Rectified Linear Activation Function (ReLU) for training the hidden layers of the neural networks. ReLU prevents an exponential growth in the computation required to operate neural networks. As we formulated the given problem as a binary classification problem, we used the Sigmoid (Logistic) activation function for the output layer. Both neural network models were trained from scratch. We used the Stochastic Gradient Descent (SGD) optimization algorithm for training the neural network models and applied a binary cross-entropy loss. Our solution was implemented using the Keras library in Python. We used the GridSearchCV class from the scikit-learn Python library. GridSearchCV enabled selection of the best parameters from a hyperparameter set during training [50]. The learning parameters used for MLICOS2 are batch size, learning rate, number of epochs and momentum. We trained our neural network models for 250 epochs with a learning rate of 0.1. We used a mini batch of 256 and 0.9 as momentum.

We set α as the threshold value for both MLICOS1 and MLICOS2. After the testing phase, the algorithm outputs the classes of users (C-1 and C-2) and the associated SINR values for each user. The simulations in NS-3 are performed until there are no users affected by the interference (*i.e.,* in the C-2 class) or no significant improvements have been achieved in the past iterations (*i.e.,* the number of users in the C-2 class remained the same).

TABLE I: Simulation Parameters

Parameter	**Value**
Number of MBS	1
Number of FBS	2
Femtocell Coverage	10m
Max. MBS Transmit Power	46 dbm
Max. FBS Transmit Power	20 dbm
Downlink Frequency	2150 MHz
Uplink Frequency	1940 MHz
Width of Band	90 MHz
Duplex Spacing	190 MHz
Number of Resource Blocks	100
Number of Subchannels	1200
Subcarrier Bandwidth	15 KHz
Mobility Model	Constant Position
Femtocell Access	Closed Access

TABLE II: Properties for the Video Used for Transmission

Parameter	**Value**
Width	1280
Height	720
Total Bitrate	1209Kbps
Frame Rate	30 fps
Total Duration	10 seconds
Total Frames	300 frames

This article has been accepted for publication in IEEE Transactions on Multimedia. This is the author's version which has not been fully edited and content may change prior to final publication. Citation information: DOI 10.1109/TMM.2022.3187607

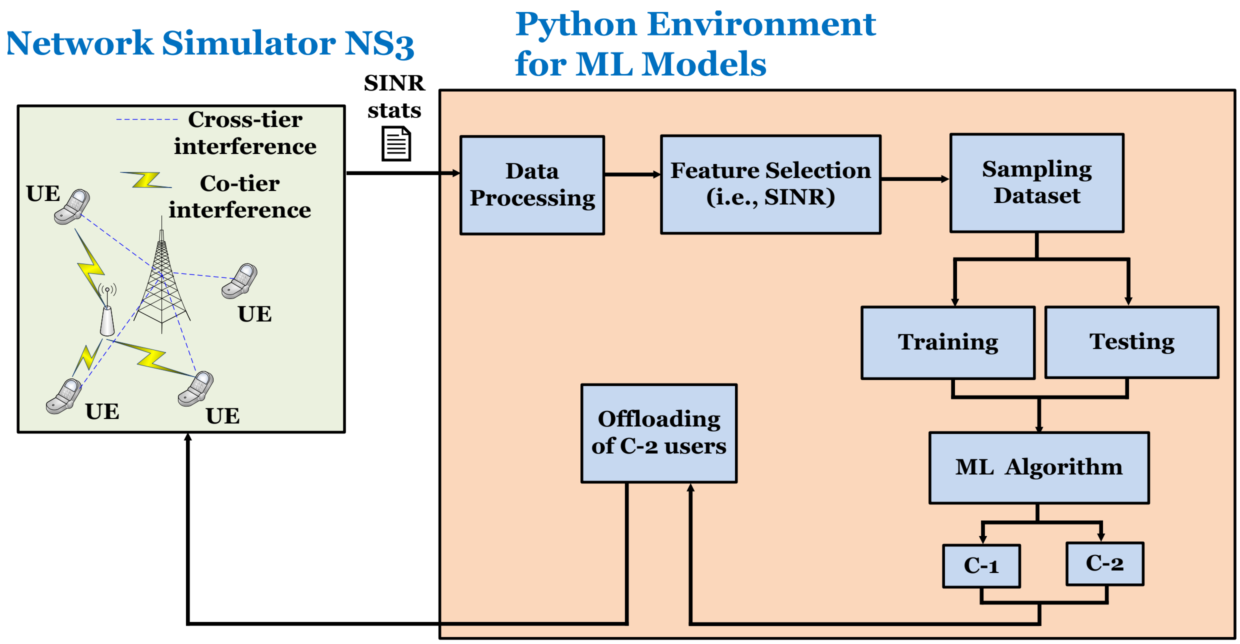

Fig. 5: Various elements of data simulation, ML algorithms, and network process

V. Performance Evaluation

We consider a heterogeneous scenario with one MBS (N_m = 1) and two FBSs (N_f = 2) along with a number of users N_u which increases linearly from 50 to 130. Gercom's Evalvid model in NS-3 is used for video transmissions. The Evalvid model transmits the video in the form of a trace file. The sender and receiver trace files are compared, allowing for the recreation of the video at the receiver end. An H.264 encoded video consisting of 300 frames with a data rate of 1200 Kbps and frame rate of 30 fps was selected for streaming. Table II presents additional video stream details.

All users are randomly allocated to the nearest FBS within the MBS coverage area. Any user between the two FBSs and MBS is subjected to strong interference. The macrocell also transmits signals in the same channel within the same area, resulting in interference. In this work, we consider only the co-tier interference between the femtocells and their associated users according to Eq. (1). Table I depicts the simulation parameters used.

The performance of the proposed scheme employing SVM and RF classifiers in turn is assessed in terms of accuracy, precision, recall and F-measure. The proposed scheme is also assessed in terms of the following QoS parameters: throughput, PLR and delay.

A. MLICOS Classifier Assessment

The classifier assessment is evaluated based on the following metrics:

1) Accuracy: defined as the percentage of correctly classified predictions (CP), divided by the total number of predictions (T) made by a model in a dataset.

$$Accuracy = \frac{CP}{T} \tag{18}$$

where CP and T are defined as:

$$CP = TP + TN \tag{19}$$

$$T = TP + TN + FP + FN \tag{20}$$

where TP denotes true ositive, FP means false positive, TN represents true negative and FN is false negative. TP and TN correctly indicate the presence or absence of some characteristics, whereas FP and FN incorrectly identify the presence or absence of the same characteristics, respectively. In this paper, the characteristics are the interference levels and TP, FP, TN and FN are computed based on the correct and incorrect classification of a user based on interference level when comparing the model prediction with the actual classification values.

Fig. 6a depicts the accuracy for MLICOS employing SVM, RF, ANN, and CNN, respectively. We observe that the **CNN achieves the highest accuracy (99.02%), followed by RF (98.91%), ANN (96.38%), and SVM (95.47%).**

2) Recall: defined as the percentage of TP predictions by the total number of actual positive predictions TP+FN.

$$Recall = \frac{TP}{TP + FN} \tag{21}$$

Fig. 6b illustrates the recall in terms of percentage for MLICOS employing SVM, RF, ANN, and CNN. We observe that the **CNN provides the highest recall (99.11%), followed by RF (98.04%), ANN (95.82%), and SVM (91.63%).**

3) Precision: defined as the percentage of TP predictions by the total number of positive predictions TP+FP.

$$Precision = \frac{TP}{TP + FP} \tag{22}$$

The precision for MLICOS employing SVM, RF, ANN, and CNN is shown in Fig. 7a. **We observe that the CNN achieves the highest precision (98.63%), followed by RF (97.56%), ANN (96.27%), and SVM (93.24%).**

This article has been accepted for publication in IEEE Transactions on Multimedia. This is the author's version which has not been fully edited and content may change prior to final publication. Citation information: DOI 10.1109/TMM.2022.3187607

TABLE III: Machine Learning Model vs. Performance Metrics

Model	Accuracy	Recall	Precision	F-measure
SVM	95.47%	91.63%	93.24%	92.42%
RF	98.91%	98.04%	97.56%	97.79%
ANN	96.38%	95.82%	96.27%	96.04%
CNN	99.02%	99.11%	98.63%	98.86%

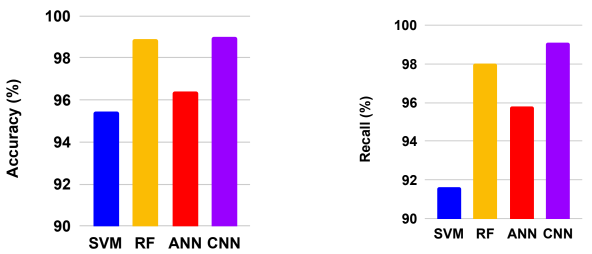

(a) Accuracy vs. Model

(b) Recall vs. Model

Fig. 6: Accuracy and Recall

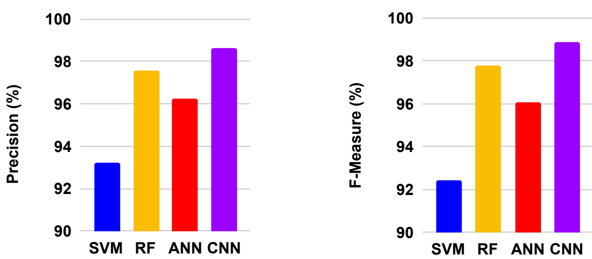

(a) Precision vs. Model

(b) F-Measure vs. Model

Fig. 7: Precision and F-Measure

4) F-Measure (FM): defined as the harmonic mean of precision and recall and is given by:

$$FM = 2 * \frac{Precision * Recall}{Precision + Recall} \tag{23}$$

Fig. 7b shows the F-measure for the four classifier models used in the proposed MLICOS algorithm. **We observe that when the CNN is employed, the results include the highest F score (98.86%), followed by the scenario when RF (97.79%), ANN (96.04%), and SVM (92.42%) are used respectively.** Table III summarizes the assessment results. We propose two versions of MLICOS, namely, **MLICOS1** and **MLICOS2**. The former uses SVM and RF as classification models, while the latter uses the ANN and CNN. Based on the superior performance results achieved and presented in Table III, the RF-based MLICOS1 and the CNN-based MLICOS2 were selected to be compared in the testing phase.

B. QoS Assessment

When testing the performance of MLICOS1 and MLICOS2, it was compared with that of the Proportional Fair (PF), Variable Radius + Proportional Fair (VR+PF) [28], and a Cognitive Approach (CA) [23]. The performance was assessed in terms of QoS parameter throughput, delay and PLR.

Fig. 8 illustrates the average throughput with respect to the number of users for the three schemes. For instance, MLICOS1 using RF achieved an average throughput of 6500 Kbps per user, which was **83.88%**, **66.79%** and **41.52%** higher than the values output by the PF, VR + PF, and CA schemes, respectively. On the other hand, using CNN-based MLICOS2, the achieved average throughput was 6900 Kbps per user, which was **84.61%**, **68.28%**, **44.15%** and **4.51%** higher than the throughput recorded when the PF, VR + PF, CA and MLICOS1 schemes were employed, respectively.

TABLE IV: Comparison between QoS results when using PF, VR+PF, CA and MLICOS (both versions) schemes

Users	Scheme	Throughput (Kbps)	Delay (ms)	PLR (%)
50	PF	3974.54	440.38	39.61
	VR+PF	5951.78	327.51	22.37
	CA	6757.14	106.47	16.44
	MLICOS1	7859.65	10.742	0.15
	MLICOS2	8017.68	9.82	0.12
70	PF	3765.20	558.72	65.55
	VR+PF	5514.54	401.57	48.91
	CA	6385.51	125.86	39.72
	MLICOS1	7504.77	33.43	0.72
	MLICOS2	7781.24	29.57	0.57
90	PF	2282.66	681.71	78.66
	VR+PF	4879.23	498.67	62.63
	CA	5417.71	161.55	58.2
	MLICOS1	7115.92	58.15	1.21
	MLICOS2	7369.66	52.14	0.82
110	PF	2041.24	954.1	87.66
	VR+PF	3597.72	513.56	78.711
	CA	4971.89	214.62	71.56
	MLICOS1	6904.88	75.41	4.97
	MLICOS2	7018.52	70.93	3.75
130	PF	1050.78	1029.58	98.57
	VR+PF	2165.68	647.01	89.27
	CA	3813.64	302.42	82.92
	MLICOS1	6521.54	105.94	5.53
	MLICOS2	6828.92	96.58	4.38

Fig. 9 depicts PLR as a function of the number of users. We observe that PLR per user remained under 6% when using both MLICOS1 and MLICOS2. The value obtained by MLICOS1 was **96.912%**, **87.69%**, and **63.22%** lower than the results of PF, VR + PF, and CA, respectively. The values obtained using the MLICOS2 scheme were **97.01%**, **88.21%**, **64.13%** and **9.97%** lower than the results recorded when employing PF, VR+PF, CA, and MLICOS1, respectively.

Fig. 10 shows the delay with respect to the number of users. Using MLICOS1, the average delay per user was less than 110 ms, compared to larger values achieved by the PF, VR + PF, and CA schemes. The values obtained were **88.73%**, **78.68%**, and **46.17%** lower than the delays incurred by PF, VR + PF, and CA, respectively. With MLICOS2, the average delay per user was less than 100 ms, much shorter than the large delay values achieved by PF, VR + PF, CA, and MLICOS1. The values obtained were **90.25%**, **80.04%**, **47.68%** and **10.68%** lower than the delays of PF, VR+PF, CA, and MLICOS1, respectively.

Based on the above QoS results, MLICOS2 performs better than the MLICOS1. Hence, MLICOS2 can be used in a real-world scenario with high dimensional datasets and can perform better than other classification models in terms of accuracy, precision, recall and F-measure. Our simulation results show that the goals described in Eqs. (11), (12), and (13) are achieved by the proposed solution. Table IV presents a summary of the QoS results when using MLICOS1 and MLICOS2 along with three other solutions.

This article has been accepted for publication in IEEE Transactions on Multimedia. This is the author's version which has not been fully edited and content may change prior to final publication. Citation information: DOI 10.1109/TMM.2022.3187607

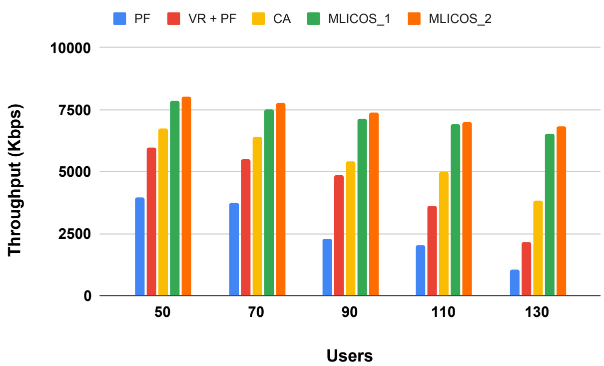

Fig. 8: Throughput vs. Number of users

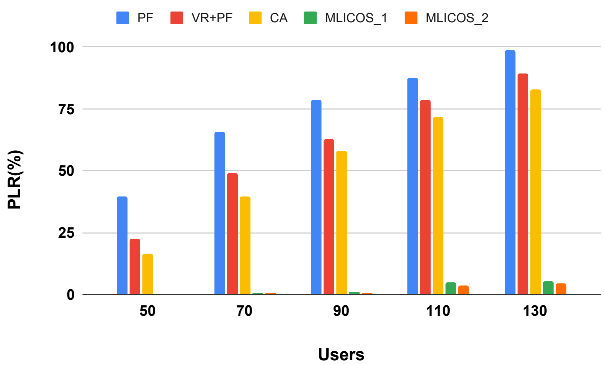

Fig. 9: PLR vs. Number of users

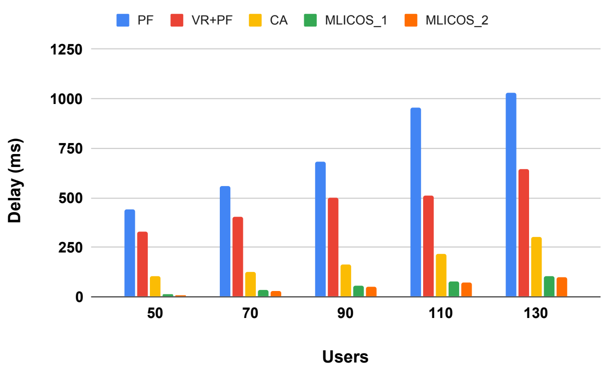

Fig. 10: Delay vs. Number of users

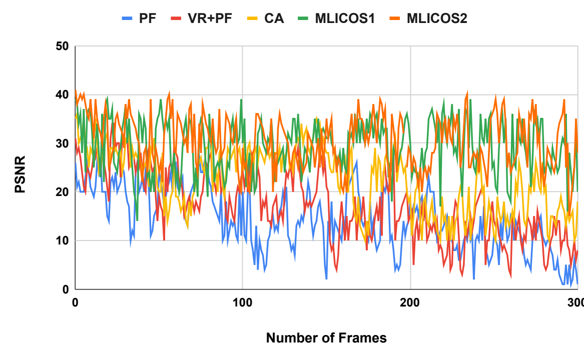

Fig. 11: PSNR Estimation

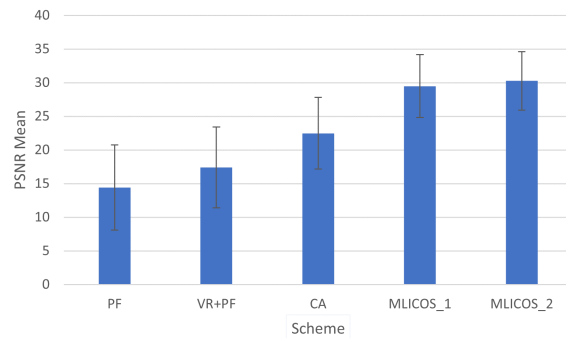

Fig. 12: Mean and Standard Deviation of PSNR

C. QoE Estimation

As illustrated in Fig. 1, we consider video streaming to be a high priority service for users. Thus, objective quality assessment of video sequences (as perceived by a user) becomes crucial. We consider Peak signal-to-noise-ratio (PSNR) as an estimation metric for the QoE. It is a signal quality metric that is computed over all pixels in the video with respect to a reference video. The PSNR value is calculated and mapped directly on the Mean Opinion Score (MOS), as specified in ITU-T J.144 standard. The PSNR estimation outcomes are shown in Fig. 11 over 300 frames for 130 users. The PSNR profiles are different for all five schemes, and the perceived quality experienced by C-2 users is much better under both versions of MLICOS. Fig. 12 shows the error bar, which uses the standard deviation as one of the uncertainties over the mean of the PSNR achieved when different schemes are used. We observe that while incurring low variations, the mean value of PSNR under MLICOS2 was **52.7%, 42.96%, 26.2% and 3.3%** higher and incurred much lower variations than what was achieved when PF, VR+PF, CA, and MLICOS1 were employed, respectively, while incurring much lower variations. The numerical results show how MLICOS2 improves the user's QoE in terms of PSNR, outperforming the other schemes.

D. Statistical Visualization

To visualize the degree of interference faced by a user under all schemes, we used the box plot (data analysis) method in R. Using this method, we can easily compare the different schemes in terms of the degree of interference experienced by C-2 users. The UIM values (according to Eq. (14)) are normalized using the min-max normalization method.

Fig. 13a, 13b, 13c, 13d and 13e show the box plots for PF, VR + PF, CA, MLICOS1 and MLICOS2, respectively. The degree of interference is indicated by values ranging between 0 and 1. When values are closer to 1, they imply that users experience high co-tier interference, whereas when values are near 0, they indicate that users are the least affected by the co-tier interference.

Fig. 13a shows that when the PF scheme is applied for 50 users, most users face very little interference, but when the number of users increases to 130, the normalized interference value for each user is very close to 1, and almost all users are affected by co-tier interference. Fig. 13b depicts the box plot visualization for the VR + PF scheme. The box plot results of the VR + PF scheme are better than those of the PF scheme. Indeed, when the number of users is below 90, most users experience low co-tier interference. Nevertheless, when the number of users increases to 130, most users experience high

This article has been accepted for publication in IEEE Transactions on Multimedia. This is the author's version which has not been fully edited and content may change prior to final publication. Citation information: DOI 10.1109/TMM.2022.3187607

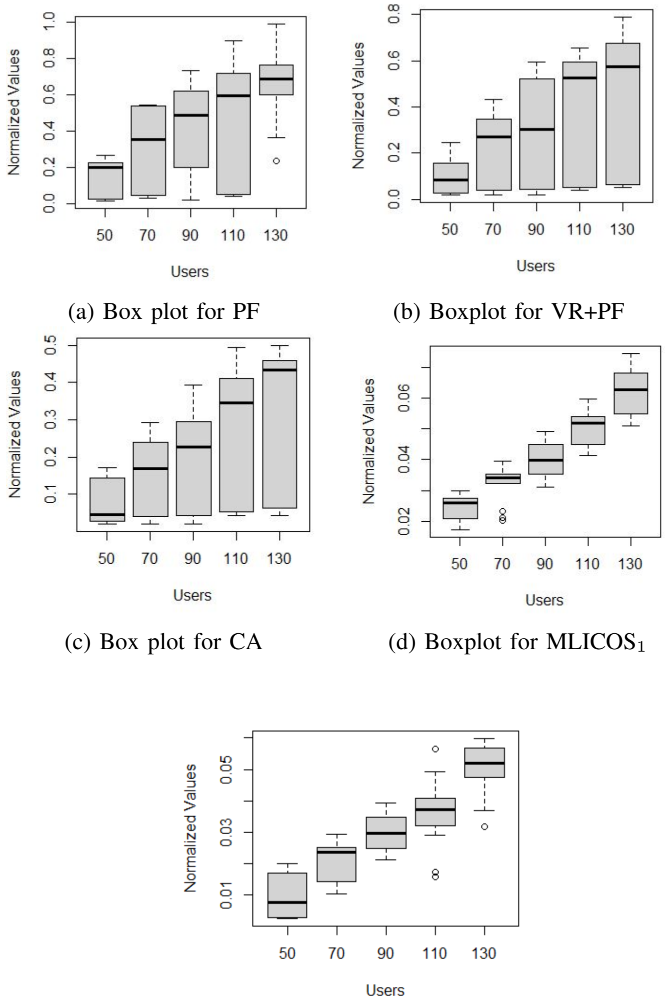

(a) Box plot for PF

(b) Boxplot for VR+PF

(c) Box plot for CA

(d) Boxplot for $MLICOS_1$

(e) Boxplot for $MLICOS_2$

Fig. 13: Degree of interference faced by users under various compared schemes. The Y axis shows the degree of interference normalized values (0 to 1 range).

co-tier interference. Fig. 13c shows the box plot for the CA scheme. When the CA scheme is deployed, we observe that when the number of users reaches 130, only 50% of users are affected by high co-tier interference. Figs. 13d and 13e illustrates the box plot for MLICOS1 and MLICOS2. We observe that users hardly experience any interference. Indeed, even when the number of users reaches 130, a tiny percentage of users experienced co-tier interference. This indicates that both versions of MLICOS maintain good QoS levels and mitigate the co-tier interference by making efficient use of resource blocks.

E. Statistical Analysis

Fig. 14 shows a direct comparison between the variability of the different schemes in terms of the mean, median, maximum value and standard deviation. In relation to measuring the degree of interference, we showed in the above section that the normalized values decide whether the user experiences high or low co-tier interference. Fig. 14 illustrates the maximum value for all schemes. In the case of PF, when there are 130 users, the ultimate value a user obtains is approximately 0.98, which is very close to 1, and most users experience high co-tier interference. The VR+PF scheme performs better than the PF scheme. When 130 users are considered, the maximum value any user faces is approximately 0.78, and the users experience high co-tier interference. For 130 users, the CA scheme gives the maximum value of 0.49, which shows that 50% of the users are still affected by high co-tier interference. MLICOS1 incurs a maximum value of approximately 0.07 whereas MLICOS2 has a value of 0.05, which is very close to 0. The medians for PF, VR+PF, CA, MLICOS1, and MLICOS2 are: 0.53, 0.32, 0.16, 0.04, and 0.03, respectively. The error bar indicates how precise the measurement is or how much is the variation from the reported value. We used the standard deviation as one of the uncertainties to plot the error bars. We can conclude from Fig. 14 that both versions of MLICOS incur much lower variations and errors than those associated with the PF, VR + PF, and CA schemes. Table V summarizes the statistical analysis for all schemes in terms of the degree of interference.

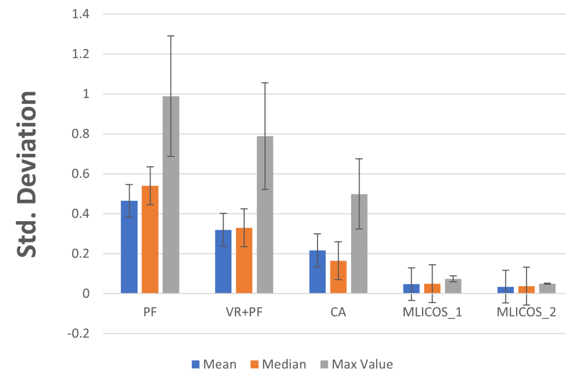

Fig. 14: Variability of different schemes

TABLE V: Comparative statistical analysis of the degree of interference when different schemes are employed

Scheme	Mean	Median	Max. Value	Std. Dev
PF	0.46	0.53	0.98	0.3
VR+PF	0.31	0.32	0.78	0.26
CA	0.21	0.16	0.49	0.17
$MLICOS_1$	0.047	0.049	0.07	0.01
$MLICOS_2$	0.035	0.037	0.05	0.002

VI. Conclusions and Future Work

In a 5G HetNet, the deployment of femtocells increases the overall network capacity. The dynamic deployment of femtocells in a HetNet leads to co-tier interference. Co-tier interference is considered one of the significant challenges, especially in urban settings. To address this problem, we proposed MLICOS, a scheme that classifies user traffic based on the interference level (*i.e.,* high and low) and offloads highly affected traffic from macrocells to nearby femtocells based on signal strength. Four ML algorithms, SVM, RF, ANN and CNN, are used in turn by the proposed solution for classification purposes. The performance of the ML-based algorithm is assessed in terms of prediction accuracy, precision, recall and F-measure. Based on the assessment, we propose two versions of MLICOS, MLICOS1 and MLICOS2. The former employs RF, while the latter uses CNN. Both versions were compared to the PF, VR + PF and CA schemes, and the results show substantial improvements in terms of QoS and QoE metrics. Simulation results also show that MLICOS2 performs better than MLICOS1. Future work will define multiple user classes while also attempting to consider the need for fast convergence. Both cross-tier and co-tier interference in a HetNet will be considered in a coordinated manner in the future.

Acknowledgements

This research was supported in part by Science Foundation Ireland under grant numbers 18/CRT/6183 (ML-LABS Centre for Research Training) and 12/RC/2289_P2 (Insight Centre for Data Analytics). For the purpose of Open Access, the author has applied a CC BY public copyright licence to any Author Accepted Manuscript version arising from this submission.

References

[1] "Cisco annual internet report - cisco annual internet report (2018–2023) white paper," Mar 2020. [Online]. Available: https://www.cisco.com/c/en/us/solutions/collateral/executive-perspectives/annual-internet-report/white-paper-c11-741490.html

[2] B. Agarwal, M. A. Togou, M. Ruffini, and G.-M. Muntean, "Pirs3a: A low complexity multi-knapsack-based approach for user association and resource allocation in hetnets," in *2021 IEEE International Conference on Communications Workshops (ICC Workshops)*, 2021, pp. 1–6.

[3] P. Schulz, H. Klessig, M. Simsek, and G. Fettweis, "Modeling qoe for buffered video streaming in interference-limited cellular networks," *IEEE Transactions on Multimedia*, vol. 23, pp. 911–925, 2021.

[4] H. Zhong, F. Wu, Y. Xu, and J. Cui, "Qos-aware multicast for scalable video streaming in software-defined networks," *IEEE Transactions on Multimedia*, vol. 23, pp. 982–994, 2021.

[5] B. Agarwal, M. A. Togou, M. Ruffini, and G.-M. Muntean, "Mitigating the impact of cross-tier interference on quality in heterogeneous cellular networks," in *IEEE Conference on Local Computer Networks (LCN)*, 2020, pp. 497–502.

[6] Y. Zhou, J. Wu, T. H. Chan, S.-W. Ho, D.-M. Chiu, and D. Wu, "Interpreting video recommendation mechanisms by mining view count traces," *IEEE Transactions on Multimedia*, vol. 20, no. 8, pp. 2153–2165, 2018.

[7] G. Yang, Y. Cao, A. Esmailpour, and D. Wang, "Sdn-based hierarchical agglomerative clustering algorithm for interference mitigation in ultra-dense small cell networks," *ETRI Journal*, vol. 40, pp. 227–236, 2018.

[8] A. A. Alotaibi and M. C. Angelides, "A serious gaming approach to managing interference in ad hoc femtocell wireless networks," *Computer Communications*, vol. 134, pp. 163–184, 2019.

[9] S. R. Samal, "Interference management techniques in small cells overlaid heterogeneous cellular networks," *J. Mobile Multimedia*, vol. 14, pp. 273–306, 2018.

[10] M. Osama, S. El Ramly, and B. Abdelhamid, "Interference mitigation and power minimization in 5g heterogeneous networks," *Electronics*, vol. 10, no. 14, 2021.

[11] S. R. Alotaibi and H. H. Sinky, "Power and radio resource management in femtocell networks for interference mitigation," *Sensors (Basel, Switzerland)*, vol. 21, 2021.

[12] R. Tian, L. Ma, Z. Wang, and X. Tan, "Cognitive interference alignment schemes for iot oriented heterogeneous two-tier networks," *Sensors*, vol. 18, p. 2548, 08 2018.

[13] S.-Y. Pyun, W. Lee, and O. Jo, "Uplink resource allocation for interference mitigation in two-tier femtocell networks," *Mobile Information Systems*, vol. 2018, pp. 1–6, 12 2018.

[14] J. Dai and S. Wang, "Clustering-based interference management in densely deployed femtocell networks," *Digital Communications and Networks*, vol. 2, 11 2016.

[15] W. Zhu, X. Wang, and W. Gao, "Multimedia intelligence: When multimedia meets artificial intelligence," *IEEE Transactions on Multimedia*, vol. 22, no. 7, pp. 1823–1835, 2020.

[16] I. Shgluof, M. Ismail, and R. Nordin, "Semi-clustering of victim-cells approach for interference management in ultra-dense femtocell networks," *IEEE Access*, vol. 5, pp. 9032–9043, 2017.

[17] H. Zhang, D. Jiang, F. Li, K. Liu, H. Song, and H. Dai, "Cluster-based resource allocation for spectrum-sharing femtocell networks," *IEEE Access*, vol. 4, pp. 8643–8656, 2016.

[18] B. Soleimani and M. Sabbaghian, "Cluster-based resource allocation and user association in mmwave femtocell networks," *IEEE Transactions on Communications*, vol. 68, no. 3, pp. 1746–1759, 2020.

[19] L.-C. Wang, S.-H. Cheng, and A.-H. Tsai, "Data-driven power control of ultra-dense femtocells: A clustering based approach," in *26th Wireless and Optical Communication Conference (WOCC)*, 2017, pp. 1–6.

[20] D. Teng and N. Ye, "Cell clustering-based resource allocation in ultra-dense networks," in *2017 3rd IEEE International Conference on Computer and Communications (ICCC)*, 2017, pp. 622–627.

[21] N. Farhan and S. Rizvi, "An interference-managed hybrid clustering algorithm to improve system throughput," *Sensors*, vol. 22, no. 4, 2022.

[22] G. Yang, A. Esmailpour, N. Nasser, G. Chen, Q. Liu, and P. Bai, "A hierarchical clustering algorithm for interference management in ultra-dense small cell networks," *IEEE Access*, vol. 8, pp. 78 726–78 736, 2020.

[23] L. Zhang, L. Yang, and T. Yang, "Cognitive interference management for lte-a femtocells with distributed carrier selection," in *2010 IEEE 72nd Vehicular Technology Conference - Fall*, 2010, pp. 1–5.

[24] G. Gür, S. Bayhan, and F. Alagöz, "Cognitive femtocell networks: an overlay architecture for localized dynamic spectrum access [dynamic spectrum management]," *IEEE Wireless Communications*, vol. 17, no. 4, pp. 62–70, 2010.

[25] M. Kamruzzaman, N. I. Sarkar, and J. Gutierrez, "A dynamic algorithm for interference management in d2d-enabled heterogeneous cellular networks: Modeling and analysis," *Sensors*, vol. 22, no. 3, 2022.

[26] W. Wang, G. Yu, and A. Huang, "Cognitive radio enhanced interference coordination for femtocell networks," *IEEE Communications Magazine*, vol. 51, no. 6, pp. 37–43, 2013.

[27] F. Liu and S. Zhao, "Statistical resource allocation based on cognitive interference estimation in ultra-dense hetnets," *IEEE Access*, vol. 8, pp. 72 548–72 557, 2020.

[28] V. Sathya, H. V. Gudivada, H. Narayanam, B. M. Krishna, and B. R. Tamma, "Enhanced distributed resource allocation and interference management in lte femtocell networks," in *2013 IEEE 9th International Conference on Wireless and Mobile Computing, Networking and Communications (WiMob)*, 2013, pp. 553–558.

[29] N. Fath, I. W. Mustika, Selo, K. Yamamoto, and H. Murata, "Optimal resource allocation scheme in femtocell networks based on bat algorithm," in *2016 22nd Asia-Pacific Conference on Communications (APCC)*, 2016, pp. 281–285.

[30] M. A. Kamal, H. W. Raza, M. M. Alam, and M. Mazliham, "Resource allocation schemes for 5g network: A systematic review," 2021.

[31] M. S. Alomari, A. Ramli, A. Sali, and r. s. a. raja abdullah, "A femtocell cross-tier interference mitigation technique in ofdma-lte system: A cuckoo search based approach," *Indian Journal of Science and Technology*, vol. 9, 01 2016.

[32] G. Chen, J. Zheng, and L. Shen, "A preset threshold based cross-tier handover algorithm for uplink co-channel interference mitigation in two-tier femtocell networks," in *2013 IEEE Global Communications Conference (GLOBECOM)*, 2013, pp. 4717–4722.

[33] M. Susanto, D. Fauzia, Melvi, and S. Alam, "Downlink power control for interference management in femtocell-macrocell cellular communication network," in *2017 15th International Conference on Quality in Research (QiR) : International Symposium on Electrical and Computer Engineering*, 2017, pp. 479–484.

[34] T. Hassan and F. Gao, "An active power control technique for downlink interference management in a two-tier macro–femto network," *Sensors*, vol. 19, p. 2015, 04 2019.

[35] M. Osama, S. El Ramly, and B. Abdelhamid, "Interference mitigation and power minimization in 5g heterogeneous networks," *Electronics*, vol. 10, no. 14, p. 1723, 2021.

[36] O. I. Ladipo and A. O. Gbenga-Ilori, "Hierarchical power control model for interference mitigation in a two – tier heterogeneous network," *Cogent Engineering*, vol. 6, no. 1, p. 1691358, 2019.

[37] Y. Chen, "Mathematical modelling of end-to-end packet delay in multi-hop wireless networks and their applications to qos provisioning," Nov 2013.

[38] B. M. Parker, S. Gilmour, J. Schormans, and H. Maruri-Aguilar, "Optimal design of measurements on queueing systems," *Queueing Syst 79*, pp. 365–390, 2015.
[39] M. Roshan, J. A. Schormans, and R. Ogilvie, "Video-on-demand qoe evaluation across different age- groups and its significance for network capacity," *EAI Endorsed Transactions on Mobile Communications and Applications*, vol. 4, no. 12, 1 2018.
[40] A. Wahab, N. Ahmad, and J. Schormans, "Statistical error propagation affecting the quality of experience evaluation in video on demand applications," *Applied Sciences*, vol. 10, no. 10, 2020.
[41] "O-ran alliance."
[42] L. M. P. Larsen, A. Checko, and H. L. Christiansen, "A survey of the functional splits proposed for 5g mobile crosshaul networks," *IEEE Communications Surveys Tutorials*, vol. 21, no. 1, pp. 146–172, 2019.
[43] B. Balasubramanian, E. S. Daniels, M. Hiltunen, R. Jana, K. Joshi, R. Sivaraj, T. X. Tran, and C. Wang, "Ric: A ran intelligent controller platform for ai-enabled cellular networks," *IEEE Internet Computing*, vol. 25, no. 2, pp. 7–17, 2021.
[44] D. Anand, M. A. Togou, and G.-M. Muntean, "A machine learning solution for automatic network selection to enhance quality of service for video delivery," in *2021 IEEE International Symposium on Broadband Multimedia Systems and Broadcasting (BMSB)*, 2021, pp. 1–5.
[45] T. J. D. Berstad, M. Riegler, H. Espeland, T. de Lange, P. H. Smedsrud, K. Pogorelov, H. Kvale Stensland, and P. Halvorsen, "Tradeoffs using binary and multiclass neural network classification for medical multidisease detection," in *2018 IEEE International Symposium on Multimedia (ISM)*, 2018, pp. 1–8.
[46] O. Owoyele, P. Pal, A. V. Torreira, D. Probst, M. Shaxted, M. Wilde, and P. K. Senecal, "Application of an automated machine learning-genetic algorithm (automl-ga) coupled with computational fluid dynamics simulations for rapid engine design optimization," 2021.
[47] R. Medar, V. S. Rajpurohit, and B. Rashmi, "Impact of training and testing data splits on accuracy of time series forecasting in machine learning," in *2017 International Conference on Computing, Communication, Control and Automation (ICCUBEA)*, 2017, pp. 1–6.
[48] M. A. Cano Lengua and E. A. Papa Quiroz, "A systematic literature review on support vector machines applied to classification," in *2020 IEEE Engineering International Research Conference (EIRCON)*, 2020, pp. 1–4.
[49] M. Chen, U. Challita, W. Saad, C. Yin, and M. Debbah, "Artificial neural networks-based machine learning for wireless networks: A tutorial," *IEEE Comms. Surveys & Tutorials*, vol. 21, no. 4, pp. 3039–3071, 2019.
[50] L. Yang and A. Shami, "On hyperparameter optimization of machine learning algorithms: Theory and practice," *Neurocomputing*, vol. 415, pp. 295–316, nov 2020.

Devanshu Anand received the B.Eng. degree in Electronics and Communication Engineering from Bangalore, India in 2020. He was a Research Intern at the Department of Electrical Engineering, Indian Institue of Technology, Kanpur. He is currently pursuing a PhD degree from the School of Electronics Engineering, Dublin City University, Dublin, Ireland. His research interests include Machine Learning solutions for rich media delivery in heterogeneous networks, resource allocation, 5G, machine learning. He is a recipient of an SFI scholarship from the ML-LABS Centre for Research Training at Dublin City University, Ireland.

Mohammed Amine Togou is a postdoctoral researcher with the SFI Insight Centre for Data Analytics at Dublin City University, Ireland. He received B.S. and M.S. degrees in computer science and computer networks from Al Akhawayn University in Ifrane, Morocco and a Ph.D. degree in computer science from the University of Montreal, Canada. He has a solid expertise in network performance optimisation, protocol design, and network security. He has published over 35 peer-reviewed scientific articles in top journals and flagship conferences. He has also served as a member of the technical programme committee of several international conferences. His research interests include 5G/6G networks, SDN-NFV, network slicing, Blockchain, IoT, cloud computing, and machine learning.

Gabriel-Miro Muntean (Senior Member, IEEE) is a Professor with the School of Electronic Engineering, Dublin City University (DCU)—Ireland and the Co-Director of the DCU Performance Engineering Laboratory. He received the Ph.D degree from DCU for his research on quality-oriented adaptive multimedia streaming in 2004. He has published over 450 papers in prestigious international journals and conferences, has authored four books and 25 book chapters, and has edited seven other books. His research interests include quality-oriented and performance related issues of adaptive multimedia delivery, performance of wired and wireless communications, energy-aware networking, and personalized technology-enhanced learning. He is an Associate Editor of the IEEE TRANSACTIONS ON BROADCASTING, the Multimedia Communications Area Editor of the IEEE COMMUNICATION SURVEYS AND TUTORIALS, and a reviewer for other important international journals, conferences, and funding agencies. He is a Senior Member of IEEE Broadcast Technology Society.